

Reactivity of Paramagnetic Fe^{II}-Bis(amidinate) Complexes

Erica Jellema,^[a] Timo J. J. Sciarone,^{*[a],[‡]} Noa M. Navarrete,^[a] Marten J. Hettinga,^[a]
Auke Meetsma,^[a] and Bart Hessen^[a]

Keywords: Iron / N ligands / Carbonylation / Lewis bases / Magnetic properties

Synthesis and characterisation of ether adducts of bis(amidinate) Fe^{II} complexes are described [amidinate = 2,6-*i*Pr₂C₆H₃-NC(Ph)N-Ph]. The isolation of these five-coordinate complexes contrasts with the homoleptic bis(amidinate) Fe complexes obtained previously with the sterically more demanding amidinate ligands 2,6-*i*Pr₂C₆H₃-NC(Ph)N-Ar (Ar

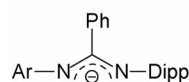
= 2,6-*i*Pr₂C₆H₃, 2,6-Me₂C₆H₃) The more accessible ether adducts show enhanced reactivity towards Lewis bases and towards the π -acid carbon monoxide. Reaction with excess amounts of CO results in carbonyl insertion into the Fe-N bonds, thereby giving rise to a diamagnetic bis(CO) adduct supported by two carbamoyl ligands.

Introduction

Amidines, [(RN)CR'(NR'')], have been used extensively as ligands for transition metals and lanthanides. With transition metals in particular, they show versatile binding modes (monodentate, bridging, chelating). The coordination mode is determined to a large extent by the nature of the C- and N-substituents. For chelating amidinate ligands, the size of the N-substituents can also influence the coordination geometry in complexes. This becomes especially apparent in homoleptic bis(amidinate)-metal complexes. In cases in which the electronic preference of the metal is not too strong, the steric demands of the ligands can actually outweigh the preference of the metal. The groups of Gambarotta and Winter have demonstrated this for Cr^{II} by using amidines with simple alkyl or silyl substituents on the C and N atoms. For the bulkier N-substituents (CMe₃ or SiMe₃), the geometry of these d⁴ complexes deviates from the planar situation found with smaller substituents (R = Cy, *i*Pr).^[1,2]

By using *o*-disubstituted aryls on the N-donor atoms, Boeré characterised a highly unusual planar Mg-bis(amidinate).^[3] This approach introduces steric protection above and below the NMN coordination plane. Our group has employed related amidinate ligands (Scheme 1) in the preparation of mono- and bis(amidinate) complexes of first-row

transition metals and Fe^{II} in particular. Thus, using benzamidinate ligands [Dipp²L]⁻ and [DippXylL]⁻, homoleptic bis(amidinate) complexes were isolated with an unusual planar geometry (Scheme 2),^[4] whereas other structurally characterised homoleptic Fe^{II}-bis(amidines) invariably exhibit tetrahedral geometries.^[5-9]



Dipp²L : Ar = 2,6-*i*Pr₂C₆H₃
DippXylL : Ar = 2,6-Me₂C₆H₃
DippPhL : Ar = C₆H₅
Dipp = 2,6-*i*Pr₂C₆H₃

Scheme 1.

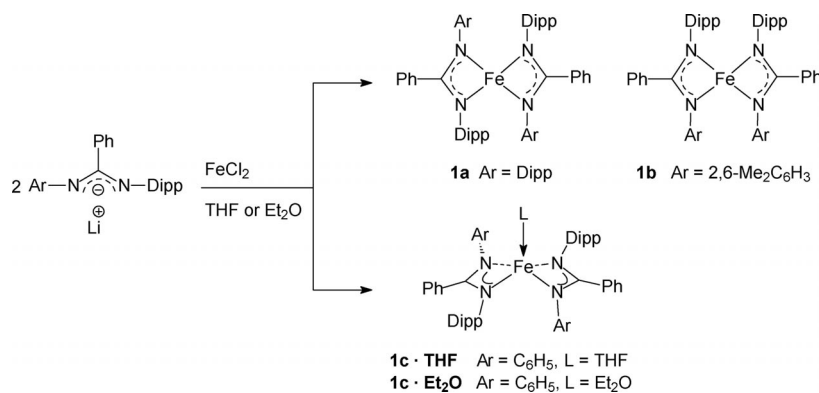
Although most studies on bis(amidinate) complexes have focussed on the relation between ligand steric bulk and coordination chemistry, interesting consequences may also be expected for the reactivity of such complexes. Particularly in mononuclear cases in which 2,6-disubstituted aryl groups are present on all four nitrogen atoms, the accessibility of the metal centre could be effectively limited. Thus, the cation [L₂ZrMe]⁺ has been reported not to interact with ethene for L = Dipp²L, whereas the analogous cation with L = DippXylL induced slow olefin polymerisation.^[10] For first-row transition metals, such shielding effects are expected to be even more pronounced due to their smaller ionic radius.

In this contribution we investigate the reactivity of Fe^{II}-bis(amidinate) complexes toward σ -base as well as π -acid ligands as a function of gradual decrease in the steric demands of the amidinate ligand. To this end, the benzamidinate [PhC(N-2,6-*i*Pr₂C₆H₃)(NPh)]⁻ ([DippPhL]⁻, Scheme 1) is introduced. The reduced steric bulk of the latter is found to open up reactivity pathways unavailable to the more crowded analogues [Dipp²L]⁻ and [DippXylL]⁻.

[a] Strating Institute for Chemistry and Chemical Engineering, University of Groningen, Nijenborgh 4, 9747 AG Groningen, The Netherlands

[‡] Present address: Polymer Chemistry Group, Eindhoven University of Technology
P. O. Box 513, 5600 MB Eindhoven, The Netherlands
Fax: +31-40-246-3966
E-mail: t.j.sciarone@tue.nl

Supporting information for this article is available on the WWW under <http://dx.doi.org/10.1002/ejic.201000717>.



Scheme 2.

Results and Discussion

Synthesis and Characterisation of Bis(amidinate) with [DippPhL][−]

Amidine ^{DippPh}LH was synthesised by standard methodology^[3] in 70% yield from *N*-(2,6-diisopropylphenyl)benzimidoyl chloride and aniline. The amidine crystallises as the *Z-anti* isomer as found by X-ray diffraction (see the Supporting Information). Also, in CDCl₃, only one isomer is observed.

In situ deprotonation (*n*BuLi) and subsequent salt metathesis with FeCl₂ in THF affords the new bis(amidinate) complex **1c·THF** (Scheme 2) after removal of the reaction solvent in vacuo followed by extraction with hexanes. The isolation of a five-coordinate adduct contrasts with the previously reported base-free complexes **1a** and **1b** and seems a direct consequence of the reduction of ligand steric bulk.

To test whether a homoleptic complex (^{DippPh}L)₂Fe could be isolated, the complexation was also performed in the weaker donor solvent diethyl ether. Again, a five-coordinate adduct, [(^{DippPh}L)₂Fe(Et₂O)] (**1c·Et₂O**) was isolated. In this case, the poor solubility of the product in alkane solvents necessitated extraction with diethyl ether. Nevertheless, the ether ligand was not lost by drying in vacuo. Attempts to remove the ether molecule from **1c·Et₂O** by vacuum sublimation at 150 °C/200 mTorr led to decomposition of the complex and afforded the parent amidine and unidentified green/brown products. Preparation of base-free **1c** by salt metathesis of Li[^{DippPh}L] with FeCl₂ in toluene was unsuccessful. Although initially a green colour reminiscent of that of (^{DippPh}L)₂Fe was observed, no Fe complex was isolated.

The solid-state structures of **1c·THF**^[11] and **1c·Et₂O** (Figure 1 and Figure 2) display approximate (noncrystallographic) C₂ symmetry with the C₂ axis passing through the Fe–O vector. The complexes are best described as square pyramidal with the four nitrogen atoms forming the basal plane and the ether ligands as apexes (τ parameter^[12] = 0.20 and 0.10 for **1c·THF** and **1c·Et₂O**, respectively). In contrast, a trigonal bipyramidal geometry was reported for the tmeda adduct [{PhC(NSiMe₃)(*N*-2,6-Me₂C₆H₃)₂Fe(κ^1 -tmeda)] (tmeda = Me₂NCH₂CH₂NMe₂).^[13] The iron

centres in the adducts **1c** are located somewhat above the N₄ basal planes [0.107(1) Å for **1c·THF**, 0.064(2) Å for **1c·Et₂O**] and the amidinate NCN planes are slightly bent away from the ether ligands. The amidinates in the basal plane assume a mutual *trans* relation, thus avoiding steric interactions between 2,6-*i*Pr₂C₆H₃ groups from the two ligands. The Fe–O distance in **1c·Et₂O** is about 0.02 Å longer than that in **1c·THF**, as expected for the weaker Lewis base. The Fe–N distances do not appear to be a direct function of the steric bulk on the nitrogen atoms, since for **1c·THF** the N^{Ph}–Fe distance is larger than N^{Dipp}–Fe, whereas the situation is reversed for **1c·Et₂O**.

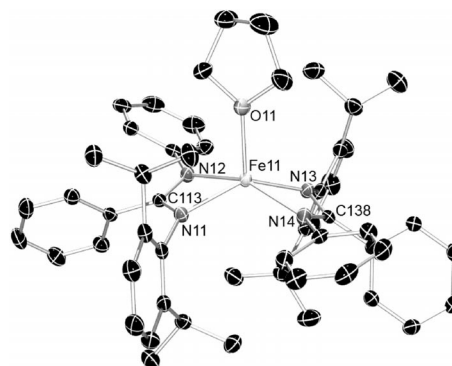


Figure 1. Molecular structure of **1c·THF** (50% thermal ellipsoids). Selected bond lengths [Å] and angles [°]: Fe11–O11 2.0714(14), Fe11–N11 2.1090(16), Fe11–N12 2.1304(15), Fe11–N13 2.1182(15), Fe11–N14 2.1329(15), N11–C113 1.326(2), N12–C113 1.334(2), N13–C138 1.332(2), N14–C138 1.335(2); O11–Fe11–N11 104.63(6), O11–Fe11–N12 98.24(6), O11–Fe11–N13 111.57(6), O11–Fe11–N14 105.75(6), N11–Fe11–N12 62.84(6), N11–Fe11–N13 143.80(6), N11–Fe11–N14 108.11(6), N12–Fe11–N13 110.18(6), N12–Fe11–N14 155.94(6), N13–Fe11–N14 62.74(6).

Magnetic susceptibility measurements show Curie–Weiss behaviour for **1c·THF** and **1c·Et₂O** in the temperature range 50–300 K with $\theta = 2.1$ K for **1c·THF** and $\theta = 4.8$ K for **1c·Et₂O** (Figure 3). The room-temperature magnetic moments of 5.3 and 5.0 μ_B , respectively, are consistent with high-spin ($S = 2$) Fe^{II} with four unpaired electrons. The effective magnetic moments are virtually temperature inde-

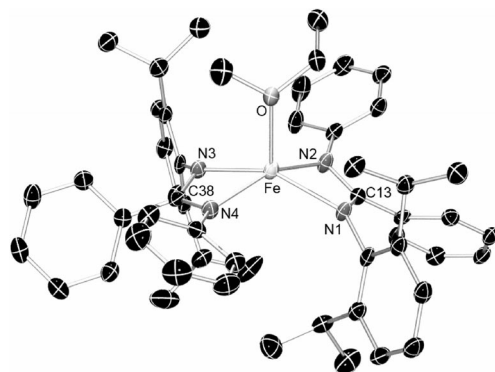


Figure 2. Molecular structure of **1c·Et₂O** (50% thermal ellipsoids). Selected bond lengths [Å] and angles [°]: Fe–O 2.0932(18), Fe–N1 2.164(2), Fe–N2 2.089(2), Fe–N3 2.157(2), Fe–N4 2.095(2), N1–C13 1.328(3), N2–C13 1.347(3), N3–C38 1.326(3), N4–C38 1.341(3); O–Fe–N1 108.26(7), O–Fe–N2 107.08(8), O–Fe–N3 102.76(7), O–Fe–N4 97.78(8), N1–Fe–N2 62.75(8), N1–Fe–N3 148.97(8), N1–Fe–N4 111.72(8), N2–Fe–N3 108.44(8), N2–Fe–N4 155.04(8), N3–Fe–N4 62.67(8).

pendent down to approximately 50 K. Below this temperature, the value of μ_{eff} drops due to zero-field splitting of the ⁵D ground state. Zero-field splitting parameters $|D| = 6.0 \text{ cm}^{-1}$ for **1c·THF** and $|D| = 8.3 \text{ cm}^{-1}$ for **1c·Et₂O** were obtained by least-squares fitting procedures using $g = 2.18$ for **1c·THF** and $g = 2.05$ for **1c·Et₂O**. These $|D|$ values are in the range usually observed for tetra- and pentacoordinate Fe^{II} complexes.^[14]

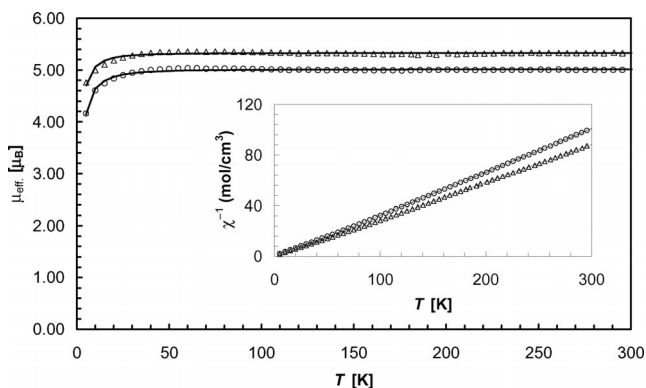


Figure 3. μ_{eff} and χ^{-1} (inset) versus T for **1c·THF** (Δ) and **1c·Et₂O** (\circ).

The paramagnetism of ether adducts **1c·THF** and **1c·Et₂O** is reflected in their ¹H NMR spectra in C₆D₆, which show broad, shifted resonances from around $\delta = +30$ to -15 ppm (Figure 4). In spite of the paramagnetism of the iron complexes, their NMR spectra were found to be quite informative.

Assignment of the resonances was aided by comparison to the spectra of **1a** and **1b**. Complete assignment, however, is precluded by the fact that some sets of magnetically in-

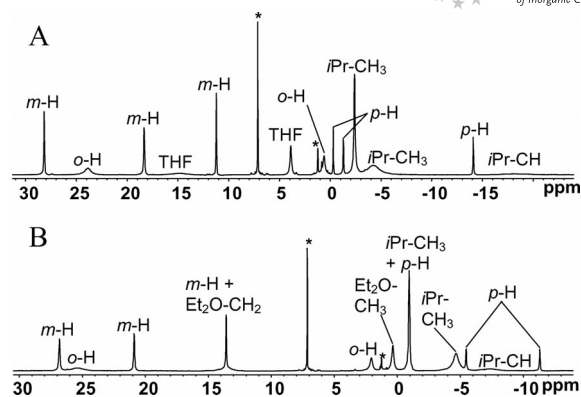
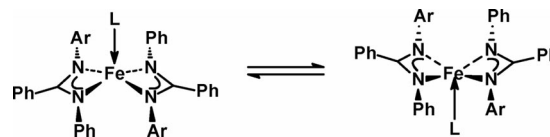


Figure 4. ¹H NMR spectra (300 MHz, C₆D₆, 298 K) of (A) **1c·THF** and (B) **1c·Et₂O**. Asterisks denote C₆D₅H and residual pentane.

equivalent protons give rise to resonances with identical integrals and similar linewidths. The C_{2h}-symmetric spectra with only two *iPr*-Me and three *m*-H resonances suggest fast site exchange of ether ligands on the ¹H NMR spectroscopic timescale (Scheme 3).



Scheme 3.

Assignment of the resonances for coordinated THF ($\delta = 14.9$ and 3.9 ppm) was confirmed by reaction with [D₈]THF (vide infra). Both adducts **1c** are thermally stable for at least 24 h at 80 °C in C₆D₆.

Reactivity towards σ Bases

The reactivity of homoleptic **1a**, **1b** and ether adducts **1c** towards σ donors was studied by ¹H NMR spectroscopy in C₆D₆. Addition of 1 equiv. [D₈]THF to **1a** or **1b**, however, does not affect their spectra. For the alkaline earth metals, the THF adducts [$\{\text{HC}(\text{NAr})_2\}_2\text{M}(\text{THF})_n$] (M = Ca, $n = 1$; M = Sr, Ba, $n = 2$; Ar = 2,6-*iPr*₂C₆H₃) have been structurally characterised.^[15] Although the shielding properties of the formamidinate resemble those of [Dⁱpp²L][−], the larger ionic radii of the divalent group II ions may enable accommodation of THF ligands.

Whereas **1a** and **1b** do not coordinate THF, reaction with the stronger Lewis base pyridine differentiates between the accessibility of the metal centres in **1a** and **1b**. The most hindered complex **1a** requires more than 1 equiv. of pyridine to observe a colour change from green to yellow. Only minor changes are visible in the ¹H NMR spectrum, even when an excess amount of pyridine is used, thereby suggesting that coordination of pyridine is weak. For the slightly more open complex **1b**, this colour change is observed with

only 1 equiv. of pyridine. The ^1H NMR spectrum of the product, tentatively formulated as $\mathbf{1b}\cdot\text{py}$, shows significant shifts and broadening of several resonances with respect to those of $\mathbf{1b}$ (see the Supporting Information). Addition of more pyridine leads to coalescence of some lines and sharpening of others, thereby suggesting that $\mathbf{1b}\cdot\text{py}$ undergoes site exchange like the ether adducts $\mathbf{1c}$, but complete assignment of the spectra proved impossible.

The more accessible iron centres in the adducts $\mathbf{1c}$ react even more readily with Lewis bases under replacement of the ether ligand. Thus, addition of $[\text{D}_8]\text{THF}$ to $\mathbf{1c}\cdot\text{Et}_2\text{O}$ leads to clean formation of $\mathbf{1c}\cdot[\text{D}_8]\text{THF}$ with liberation of diethyl ether. This experiment also permitted unambiguous assignment of the THF resonances in $\mathbf{1c}\cdot\text{THF}$. Reaction of either $\mathbf{1c}\cdot\text{THF}$ or $\mathbf{1c}\cdot\text{Et}_2\text{O}$ with 1 equiv. pyridine leads to a sole product $\mathbf{1c}\cdot\text{py}$ and is accompanied by a colour change from yellow to orange. The ^1H NMR spectrum (Figure 5A) shows four separate resonances for the *i*Pr–Me protons, which indicates magnetic inequivalence of the diastereotopic methyl groups above and below the N_4 plane. In addition, one of the *m*-aryl signals is significantly broadened. The C_{2v} -symmetric spectrum shows that site exchange for pyridine is slower than for THF on the NMR spectroscopic timescale. The fact that the pyridine ligand does exchange becomes apparent when more pyridine is added. Spectra that result from the addition of 2 equiv. and an ex-

cess amount of $[\text{D}_5]\text{pyridine}$ are shown in parts B and C of Figure 5. Significant broadening of the *i*Pr–Me resonances is observed upon addition of 2 equiv. of pyridine, whereas one of the Ar– H_m signals is sharpened. The fast exchange regime is reached with an excess amount of pyridine as evidenced by the C_{2h} -symmetric spectrum with only two diastereotopic *i*Pr–Me resonances (Figure 5, C). Removal of all volatiles in vacuo and subsequent redissolution in C_6D_6 restores the spectrum of $\mathbf{1c}\cdot\text{py}$, thereby indicating that only one pyridine is retained in the solid state. Preparative scale experiments in toluene afforded $\mathbf{1c}\cdot\text{py}$ as an orange powder. Although analytically pure material could not be obtained,

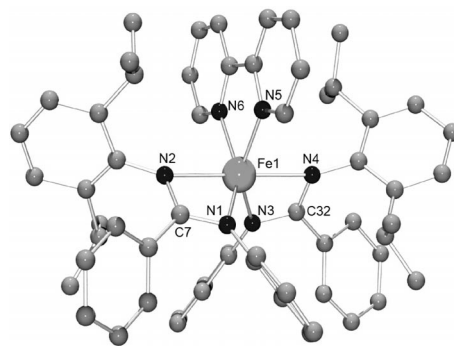


Figure 6. Molecular structure of $\mathbf{1c}\cdot\text{bpy}$.

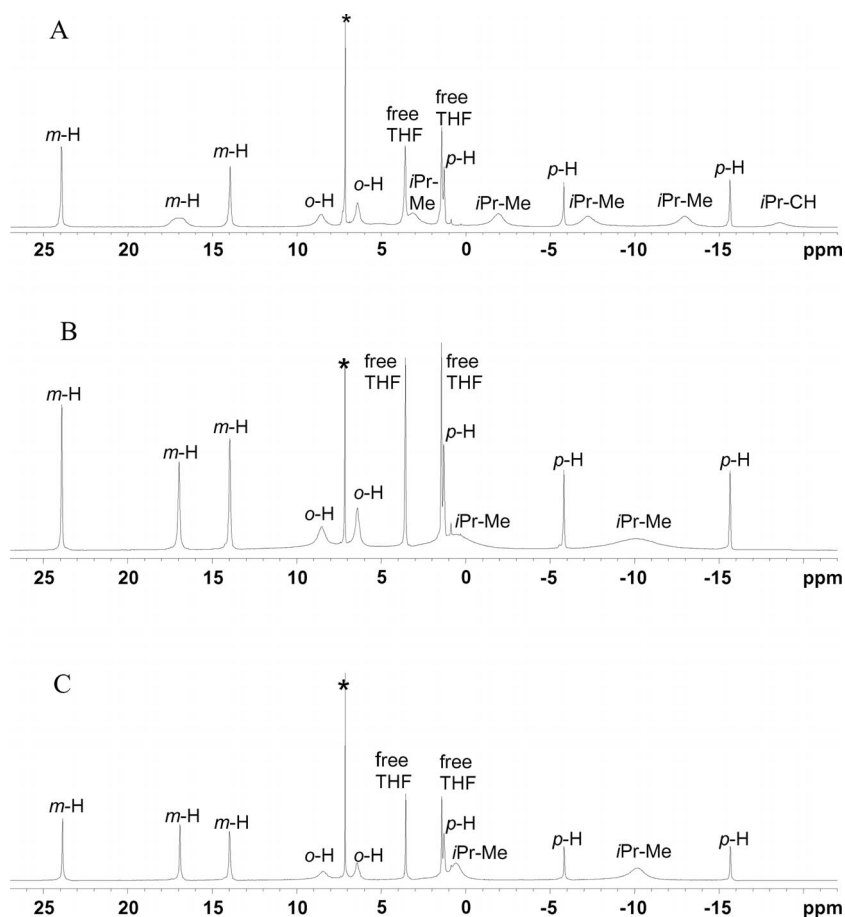


Figure 5. ^1H NMR spectra (300 MHz, C_6D_6 , 298 K) of $\mathbf{1c}\cdot\text{THF}$ + pyridine: (A) 1 equiv., (B) 2 equiv.; (C) excess amount of $[\text{D}_5]\text{pyridine}$.

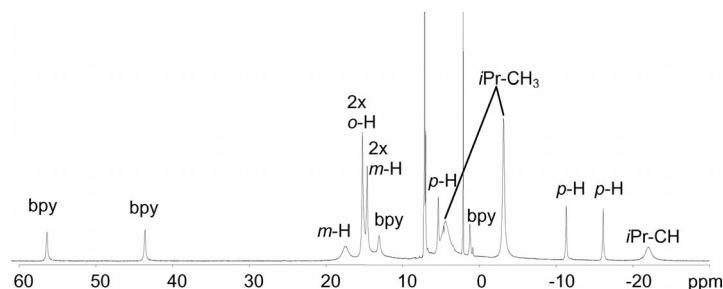


Figure 7. ¹H NMR spectrum (300 MHz, C₆D₆, 298 K) of **1c·bpy**. Asterisks denote C₆D₅H and residual toluene.

the ¹H NMR spectrum of the powder is identical to that obtained from the reaction on the scale of an NMR spectroscopy tube with 1 equiv. of pyridine.

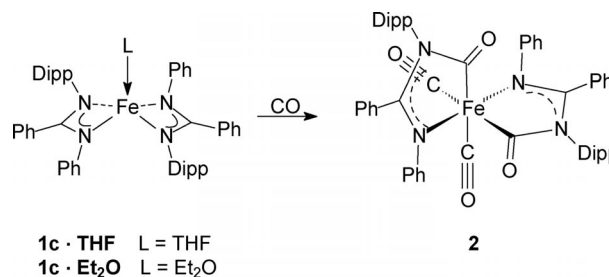
With the chelating Lewis base 2,2'-bipyridine (bpy), **1c·Et₂O** reacts in toluene to give the corresponding adduct. Dark green crystals of **1c·bpy** could be isolated in 64% yield. The molecular structure (Figure 6) shows a pseudo-octahedral coordination environment with the nitrogen atoms bearing the *N*-2,6-*i*Pr₂C₆H₃ substituents in a *trans* arrangement. Unfortunately, no crystals of sufficient quality were obtained, but the X-ray structure serves to confirm the connectivities of the non-hydrogen atoms. The asymmetric unit consists of one molecule of **1c·bpy** and highly disordered toluene molecules.

Six-coordinate **1c·bpy** is paramagnetic and magnetic measurements (superconducting quantum interference device, SQUID) indicate a room-temperature magnetic moment of 4.9 μ_B, consistent with 4 unpaired electrons (high-spin Fe^{II}). The paramagnetic ¹H NMR spectrum shows resonances from δ = +60 to -20 ppm and tentative assignments were made (Figure 7). Most amidinate protons are observed around the shifts for the related adducts **1c·L** (L = THF, Et₂O, py). Two characteristic resonances attributed to the bpy ligand are found further downfield at δ = 56.4 and 43.6 ppm.

Reactivity towards π Acids

To probe the reactivity of the bis(amidinate) complexes **1** towards π-acid ligands, their reactivity towards carbon monoxide was studied. Exhaustive carbonylation often converts paramagnetic bis(amidinate)-Fe^{II} complexes into the corresponding 18-electron bis-CO adducts.^[8,9,16,17] On account of their diamagnetism, these are amenable to NMR spectroscopic structure analysis. The sterically encumbered complexes **1a** or **1b**, however, fail to react with an excess amount of carbon monoxide (1 atm.) in C₆D₆, possibly due to the inaccessibility of the iron centres. Incomplete carbonylation due to inaccessibility of the Fe centre has been reported previously for Kawaguchi's bis(amidinate)-diiron complex.^[9] In this dimer, only one of the two iron centres was found to react with CO as a result of a more sterically hindered conformation induced by carbonylation of the first Fe centre.

The influence of steric bulk in **1a** and **1b** becomes apparent when the ether adducts of **1c** are treated with CO under the same conditions. The more accessible Fe centres in **1c·THF** and **1c·Et₂O** react rapidly, as indicated by a colour change from greenish yellow to red. After three days the colour changes to yellow again and the diamagnetic compound **2** is formed quantitatively (Scheme 4).



Scheme 4.

On a preparative scale, the final product **2** can be isolated in 33% yield as a yellow powder. It was characterised by standard spectroscopic methods and combustion analysis. An X-ray structure confirmed the formulation of **2** as a bis-(carbamoyl) complex that results from the uptake of 4 equiv. of CO. In addition to the two terminal carbonyl ligands, two more CO molecules are inserted into the amidinate Fe–N bonds. Carbonyl insertion is relatively common for Fe and Co amidinates with bulky substituents.^[16,18,19] The regiochemistry seems to be determined by steric factors as insertion usually occurs next to the nitrogen that carries the most sterically demanding substituent.^[17] Attempts to characterise the red intermediate {presumably the bis-CO adduct [(^{Dipp}Ph₂L)₂Fe(CO)₂]} were unsuccessful. Treatment of **1c·Et₂O** with 2 equiv. CO in C₆D₆ generated a red solution, but ¹H NMR spectroscopic analysis showed no other species than unreacted **1c·Et₂O** and **2**.

The solid-state structure of **2** (Figure 8) shows a pseudo-octahedrally coordinated iron centre ligated by two κ²-*N,C*-carbamoyl ligands and two terminal CO ligands in a *cis* configuration. The structure has approximate (non-crystallographic) C₂ symmetry with the C₂ axis bisecting the angle between the two terminal carbonyls. In contrast to

the parent ether adducts, in which identical C–N distances were observed in the amidinate ligands (ca. 1.33 Å), these distances differ significantly in the carbamoyl moieties in **2** (ca. 1.36 and 1.30 Å). However, the (near) planarity of all carbon and nitrogen atoms in the carbamoyl rings (sum of angles around C = 360°, sum of angles around N = 357.6–359.6°) indicates significant conjugation. The bite angle of the carbamoyl chelate is approximately 82°, comparable to the Fe^{II}–carbamoyl chloride complex [κ^3 -{Me₂N(CH₂)₂NC(Ph)N(Ar)C(O)}FeCl(CO)₂] (ca. 85°).^[17]

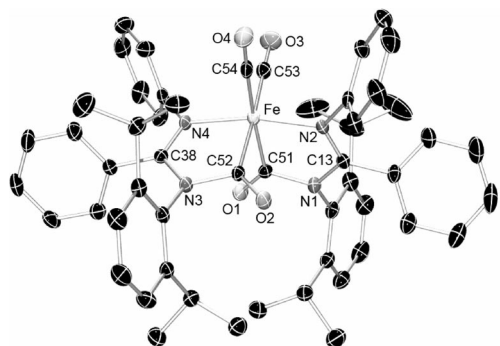


Figure 8. Molecular structure of **2** (30% thermal ellipsoids). Selected bond lengths [Å] and angles [°]: Fe–N2 1.961(3), Fe–N4 1.960(3), Fe–C51 1.953(3), Fe–C52 1.958(3), Fe–C53 1.810(4), Fe–C54 1.809(4), N1–C13 1.367(4), N2–C13 1.304(5), N3–C38 1.362(4), N4–C38 1.298(4), O1–C51 1.209(4), O2–C52 1.211(4), O3–C53 1.142(5), O4–C54 1.144(5); N2–Fe–N4 169.03(10), N2–Fe–C51 81.53(13), N2–Fe–C52 90.38(13), N2–Fe–C53 92.83(14), N2–Fe–C54 93.33(13), N4–Fe–C51 90.24(13), N4–Fe–C52 81.58(13), N4–Fe–C53 94.74(14), N4–Fe–C54 94.29(13), C51–Fe–C52 84.58(12), C51–Fe–C53 92.22(15), C51–Fe–C54 173.31(15), C52–Fe–C53 175.09(15), C52–Fe–C54 91.20(15), C53–Fe–C54 92.31(17).

NMR and IR spectroscopy for diamagnetic **2** are consistent with the *C*₂ symmetry observed in the solid state. ¹³C NMR spectroscopic resonances for the terminal carbonyls and the carbamoyl carbonyls are found at δ = 219.9 and 209.4 ppm, respectively. The ¹H NMR spectrum indicates hindered rotation of the 2,6-*i*Pr₂C₆H₃ group around the N–C_{ipso} bond. The IR spectrum shows strong absorptions at 2020 and 1961 cm^{−1} for the terminal carbonyls, whereas the CO stretching band of the carbamoyl is found at 1659 cm^{−1}. Similar values were found for other Fe^{II}–carbamoyl complexes.^[16,17]

Conclusion

The use of *o*-disubstituted aryls 2,6-R₂C₆H₃ as nitrogen substituents in bis(benzamidinate)–Fe^{II} complexes can render the metal centre virtually inaccessible to Lewis bases. Stepwise reduction of the size of R, however, gradually exposes the Fe^{II} nucleus and restores much of the reactivity common to more open Fe^{II}–amidinate complexes. Thus,

five- and six-coordinate Lewis base adducts can be obtained as well as a bis(carbamoyl) complex that results from carbonyl insertion. The accommodation of a fifth ligand, however, is also a function of the strength of the added Lewis base.

Experimental Section

General: All manipulations, except for amidine synthesis, were carried out under a dry nitrogen atmosphere using standard glovebox, Schlenk and vacuum-line techniques. Pentane, hexanes and toluene were passed over columns of Al₂O₃ (Fluka), BASF-R3-11-supported Cu oxygen scavenger and molecular sieves (Aldrich, 4 Å). THF and Et₂O (Aldrich, anhydrous, 99.8%) were dried by percolation with Al₂O₃ (Fluka). [D₈]THF and C₆D₆ were distilled from Na/K. [D₅]Pyridine (Acros) was used as received.

Starting Materials: Pyridine (Merck) was distilled from calcium hydroxide. 2,2′-Bipyridine (Merck, 99.5%), aniline, triethylamine, *n*BuLi (2.5 M in hexanes) (Acros) and CO (Praxair, 99.997%) were used as received. FeCl₂,^[20] [Dipp²L]₂Fe (**1a**)^[4] and [Dipp^{Xyl}L]₂Fe (**1b**)^[4] were prepared according to literature procedures.

Instrumentation: ¹H and ¹³C{¹H} NMR spectra were recorded at ambient temperature with a Varian VXR 300 spectrometer operating at 299.968 MHz (¹H) and a Mercury Plus 400 operating at 100.573 (¹³C{¹H}) and 399.931 MHz (¹H). NMR spectra were referenced internally using the residual solvent resonances (CHCl₃, δ = 7.26 ppm; C₆D₅H, δ = 7.15 ppm) relative to Si(CH₃)₄ (δ = 0 ppm). Proton NMR spectroscopic data for paramagnetic compounds are listed as δ [ppm] ($\Delta\nu_{1/2}$ [Hz], integral, tentative assignment). IR spectra were recorded with a 4020 Mattson Instruments FTIR spectrophotometer using nujol mulls between KBr discs. Elemental analyses were performed at the Microanalytical Department of the University of Groningen or by H. Kolbe, Mikroanalytisches Laboratorium, Mülheim an der Ruhr. Reported values are the average of two independent determinations. MS spectra were obtained with a Jeol JMS-600 spectrometer in electron ionisation (EI) mode.

***N*-Phenyl-*N'*-(2,6-diisopropylphenyl)benzamidinate (Dipp^{Pb}LH):** A solution of aniline (2.46 mL, 27 mmol), triethylamine (3.0 mL) and *N*-(2,6-diisopropylphenyl)benzimidoyl chloride (8.54 g, 27 mmol) in toluene (100 mL) was heated at reflux for 24 h. The mixture was washed with water (3×) and with a saturated solution of NaCl. Toluene was removed in vacuo. The solid was dissolved in ethanol and dried in vacuo to remove residual toluene. After recrystallisation from ethanol/water, white crystals were obtained (6.70 g, 19 mmol, 70%). ¹H NMR (200 MHz, CDCl₃, 298 K): δ = 7.63–6.27 (m, 13 H, Ar-CH), 3.16–3.23 (sept., *J* = 6.6 Hz, 2 H, *i*Pr-CH), 1.24 (d, *J* = 6.6 Hz, 12 H, *i*Pr-CH₃) ppm. ¹³C{¹H} NMR (75 MHz, CDCl₃, 298 K): δ = 153.75, 140.11, 139.06, 135.03, 129.73, 128.86, 128.71, 128.26, 123.57, 122.48, 28.16 (*i*Pr-CH), 23.92, 23.53 (2× *i*Pr-CH₃) ppm. IR (KBr): $\tilde{\nu}$ = 3359 (s, N–H), 3062 (m), 3055 (m), 3044 (m), 2921 (s), 2910 (s), 1669 (w), 1637 (s), 1597 (s), 1587 (s), 1579 (m), 1496 (s), 1448 (s), 1436 (m), 1414 (m), 1359 (m), 1343 (s), 1329 (s), 1303 (m), 1289 (m), 1261 (w), 1253 (m), 1244 (m), 1234 (m), 1194 (m), 1178 (w), 1109 (w), 1093 (m), 1075 (m), 1059 (w), 1043 (w), 1028 (w), 959 (w), 936 (w), 902 (m), 834 (w), 809 (w), 803 (w), 788 (w), 768 (s), 758 (s), 737 (s), 702 (s), 692 (s), 558 (w), 509 (w), 490 (m) cm^{−1}. HRMS (EI): calcd. for C₂₅H₂₈N₂: 356.2252; found 356.2240.

Preparation of Li^[Dipp^{Ph}]L₂: *N*-Phenyl-*N'*-(2,6-diisopropylphenyl)-benzamidinate (1.00 g, 2.74 mmol) was treated with *n*-butyllithium (1.1 mL, 2.5 M in hexanes, 2.8 mmol) in diethyl ether. After stirring for 0.5 h at room temperature, the solvent was removed in vacuo. The product was suspended in pentane and subsequently dried in vacuo to remove residual volatiles; yield 0.96 g (2.64 mmol, 96%). ¹H NMR (300 MHz, [D₈]THF/C₆D₆, 298 K): δ = 7.23–6.55 (m, 13 H, Ar-CH), 3.55 (septet, *J* = 7.0 Hz, 2 H, *i*Pr-CH), 1.17 (d, *J* = 7.0 Hz, 6 H, *i*Pr-CH₃), 1.03 (d, *J* = 7.0 Hz, 6 H, *i*Pr-CH₃) ppm. ¹³C{¹H} NMR (75 MHz, [D₈]THF/C₆D₆, 298 K): δ = 178.10 (NCN), 160.85, 155.13, 140.97, 137.27, 131.02, 128.36, 127.46, 127.31, 123.67, 122.81, 121.58, 116.94, 28.39 (*i*Pr-CH), 25.30, 23.03 (2 × *i*Pr-CH₃) ppm.

Preparation of [Dipp^{Ph}L₂Fe(THF)] (1c·THF): *n*BuLi (2.1 mL, 2.5 M in hexane, 5.2 mmol) was added dropwise over 30 min at room temperature to a solution of *N*-phenyl-*N'*-(2,6-diisopropylphenyl)-benzamidinate (1.86 g, 5.2 mmol) in 30% THF/pentane. The solvents were removed in vacuo and the product was dissolved in pentane (20 mL). The pentane was removed in vacuo. The lithium *N*-phenyl-*N'*-(2,6-diisopropylphenyl)benzamidinate in THF (15 mL) was added to a stirred suspension of FeCl₂ (0.33 g, 2.6 mmol) in THF (15 mL) at room temperature. The colour of the mixture changed from transparent through yellow/green to brown. The reaction mixture was stirred for 2 h. The solvents were removed and the remainder was suspended in pentane. The pentane was removed under reduced pressure and the solid was extracted with hexane (40 mL). The obtained brown solution was decanted from the yellow solid. The solid was washed with pentane and dried in vacuo; yield 0.76 g (35%). ¹H NMR (300 MHz, C₆D₆, 298 K): δ = 28.2 (23, 4 H, Ar-H_m), 23.9 (216, 4 H, Ar-H_o), 18.4 (32, 4 H, Ar-H_m), 14.9 (979, 2 H, THF), 11.2 (20, 4 H, Ar-H_m), 3.9 (53, 4 H, THF), 0.6 (78, 4 H, Ar-H_o), -0.3 (19, 2 H, Ar-H_p), -1.3 (23, 2H Ar-H_p), -2.4 (43, 12 H, *i*Pr-CH₃), -4.2 (488, 12 H, *i*Pr-CH₃), -14.1 (22, 2 H, Ar-H_p), -18.2 (1488, 2 H, *i*Pr-CH) ppm. IR (KBr): ν̄ = 3053 (m), 3049 (m), 3035 (m), 3012 (m), 2965 (s), 2961 (s), 2957 (s), 2951 (s), 2948 (s), 2944 (s), 2941 (s), 2938 (s), 2935 (s), 2931 (s), 2927 (s), 2920 (s), 2913 (s), 2910 (s), 2905 (s), 2902 (s), 2898 (s), 2891 (s), 2881 (s), 2871 (s), 2863 (s), 2858 (s), 1638 (w), 1592 (m), 1579 (m), 1491 (s), 1467 (s), 1454 (s), 1438 (s), 1435 (s), 1360 (s), 1340 (m), 1319 (m), 1288 (m), 1269 (m), 1253 (m), 1237 (m), 1190 (w), 1179 (w), 1173 (w), 1157 (w), 1152 (w), 1121 (m), 1100 (m), 1075 (w), 1054 (w), 1040 (w), 1026 (s), 997 (w), 954 (m), 949 (w), 914 (w), 871 (m), 787 (m), 765 (s), 731 (m), 702 (s), 696 (s), 560 (w), 507 (w) cm⁻¹. μ_{eff} (SQuID, 298 K) = 5.3 μ_B. C₅₄H₆₂FeN₄O (838.96): calcd. C 77.31, H 7.45, N 6.68; found C 77.41, H 7.38, N 6.64.

Preparation of [Dipp^{Ph}L₂Fe(Et₂O)] (1c·Et₂O): *n*-Butyllithium (1.8 mL, 2.5 M in hexanes, 4.4 mmol) was added dropwise over 30 min at room temperature to a solution of *N*-phenyl-*N'*-(2,6-diisopropylphenyl)benzamidinate (1.56 g, 4.4 mmol) in diethyl ether (30 mL). The solvent was removed in vacuo and the remainder was suspended in pentane and dried (2 ×) to remove residual volatiles. The lithium *N*-phenyl-*N'*-(2,6-diisopropylphenyl)benzamidinate was dissolved in diethyl ether (15 mL) and added to a stirred suspension of FeCl₂ (0.28 g, 2.2 mmol) in diethyl ether (20 mL) at room temperature. The colour of the mixture changed from transparent through yellow and green to brown. The reaction mixture was stirred for 16 h and subsequently the solid was extracted with diethyl ether. The greenish yellow solution in diethyl ether was concentrated and stored at -20 °C to afford yellow crystals (1.34 g, 1.6 mmol, 73%). ¹H NMR [300 MHz, C₆D₆ (36 mm), 298 K]: δ = 26.8 (55, 4 H, Ar-H_m), 25.4 (117, 4 H, Ar-H_o), 21.0 (37, 4 H, Ar-H_m), 13.7 (31, 4 H, Ar-H_m overlapping with broad signal for Et₂O-CH₂), 2.2 (111, 4 H, Ar-H_o), 0.6 (78, 6 H, Et₂O-Me), -0.9 (38, 14

H, *i*Pr-CH₃ + Ar-H_p), -4.7 (176, 12 H, *i*Pr-CH₃), -5.6 (48, 2 H, Ar-H_p), -7.0 (241, 2 H, *i*Pr-CH), -11.2 (55, 2 H, Ar-H_p) ppm. The ¹H NMR spectrum of 1c·Et₂O is concentration dependent. The resonances at δ = 25.4, 13.7 and -0.9 ppm shift to lower field at higher concentrations. IR (KBr): ν̄ = 3055 (m), 3015 (m), 1594 (m), 1579 (s), 1492 (s), 1465 (s), 1426 (s), 1380 (s), 1360 (s), 1319 (s), 1288 (m), 1270 (m), 1254 (m), 1237 (m), 1189 (m), 1172 (m), 1151 (w), 1121 (w), 1101 (m), 1088 (w), 1075 (w), 1042 (m), 1027 (m), 996 (w), 950 (m), 936 (w), 917 (w), 896 (w), 831 (w), 803 (w), 790 (m), 766 (s), 732 (m), 698 (s), 576 (w), 562 (w), 510 (w), 497 (w) cm⁻¹. μ_{eff} (SQuID, 298 K) = 5.0 μ_B. C₅₄H₆₄FeN₄O (840.97): calcd. C 77.12, H 7.67, N 6.66; found C 76.97, H 7.62, N 6.56.

Reaction of [Dipp^{Ph}L₂Fe] (1a) with Pyridine: A green solution of [Dipp^{Ph}L₂Fe] (11 mg, 0.01 mmol) in C₆D₆ (ca. 0.4 mL) was reacted with pyridine (1 equiv., 1 mg, 0.01 mmol). No colour change was observed. The colour of the solution changed to yellow upon addition of a second equivalent. The colour remained yellow after subsequent addition of a few drops (excess amount) of pyridine. ¹H NMR (300 MHz, C₆D₆, 1 equiv. pyridine, 298 K): δ = 56.4 (887), 31.7 (41, 4 H), 22.2 (41, 4 H), 16.8 (22, 4 H), 14.6 (141, 12 H), 8.3, 7.6, 6.9 (pyridine), 6.4 (100, 4 H), 3.8 (97, 12 H), -2.0 (23, 2 H), -5.1 (58, 12 H), -6.2 (29, 4 H), -29.0 (249, 12 H) ppm. ¹H NMR (300 MHz, C₆D₆, 2 equiv. pyridine, 298 K): δ = 55.8 (857), 31.6 (45, 4 H), 22.1 (44, 4 H), 16.8 (25, 4 H), 14.5 (150, 12 H), 12.3 (383, 4 H), 7.7, 7.3, 6.9 (pyridine), 6.5 (107, 4 H), 3.8 (107, 12 H), -1.9 (26, 2 H), -5.0 (64, 12 H), -6.3 (31, 4 H), -28.9 (261, 12 H) ppm. ¹H NMR (300 MHz, C₆D₆, excess amount of pyridine, 298 K): δ = 36.1 (679), 27.8 (62, 4 H), 22.2 (50, 4 H), 17.5 (22, 4 H), 11.2 (130), 9.6–6.6 (br., pyridine and C₆D₅H), 3.6 (116, 12 H), -1.7 (75, 12 H), -7.2 (27, 4 H), -14.7 (928), -24.6 (225, 12 H) ppm.

Reaction of [Dipp^{Xyl}L₂Fe·C₆H₆] (1b·C₆H₆) with Pyridine: A solution of [Dipp^{Xyl}L₂Fe·C₆H₆] (12 mg, 0.01 mmol) in C₆D₆ (ca. 0.4 mL) was treated successively with 1 equiv. (1 mg, 0.01 mmol), 2 equiv. and an excess amount of pyridine. The colour of the solution changed to yellow immediately after the first equivalent of pyridine was added. ¹H NMR (300 MHz, C₆D₆, 1 equiv. pyridine, 298 K): δ (Δν_{1/2}, Hz) = 63.0 (br), 29.3 (1827), 26.2 (972), 19.8 (27), 17.6 (168), 12.5 (395), 4.2 (40), 1.1 (60), -9.5 (30), -14.0 (90), -16.8 (179) ppm. ¹H NMR (300 MHz, C₆D₆, 2 equiv. pyridine, 298 K): δ (Δν_{1/2}, Hz) = 25.9 (1128), 20.6 (23), 19.8 (73), 10.5 (256), 5.3 (21), 1.3 (70), -9.5 (30), -15.1 (36), -18.6 (66) ppm. ¹H NMR (300 MHz, C₆D₆, excess amount of pyridine, 298 K): δ (Δν_{1/2}, Hz) = 25.9 (998), 20.4 (28), 20.2 (169), 12.1–4.4 (br., overlapping with pyridine and C₆D₅H), 5.4 (44), 1.3 (95), -9.6 (37), -15.3 (39), -18.9 (76) ppm.

Reactions of [Dipp^{Ph}L₂Fe(THF)] (1c·THF) with Pyridine: A solution of [Dipp^{Ph}L₂Fe(THF)] (10 mg, 0.01 mmol) in C₆D₆ (ca. 0.4 mL) was treated with pyridine (1 mg, 0.01 mmol). The colour of the solution changed to yellow. ¹H NMR (300 MHz, C₆D₆, 1 equiv. pyridine, 298 K): δ (Δν_{1/2}, Hz) = 120.3 (448), 44.1 (190), 24.0 (22, 4 H, Ar-H_m), 16.9 (306, 4 H, Ar-H_m), 14.0 (30, 4 H, Ar-H_m), 8.6 (165, 4 H, Ar-H_o), 6.4 (92, 4 H, Ar-H_o), 3.6 (s, THF), 3.1 (351, 6 H, *i*Pr-CH₃), 1.4 (s, THF), 1.3 (24, 2 H, Ar-H_p), -1.9 (241, 6 H, *i*Pr-CH₃), -5.8 (21, 2 H, Ar-H_p), -7.2 (300, 6 H, *i*Pr-CH₃), -13.0 (280, 6 H, *i*Pr-CH₃), -15.7 (20, 2 H, Ar-H_p), -18.6 (308, *i*Pr-CH) ppm.

A solution of [Dipp^{Ph}L₂Fe(THF)] (18 mg, 0.02 mmol) in C₆D₆ (ca. 0.4 mL) was treated with pyridine (4 mg, 0.04 mmol). The colour of the solution changed to yellow immediately. ¹H NMR (200 MHz, C₆D₆, 2 equiv. pyridine, 298 K): δ = 24.2 (18, 4 H, Ar-H_m), 17.1 (23, 4 H, Ar-H_m), 14.0 (21, 4 H, Ar-H_m), 8.9 (128, 4 H, Ar-H_o), 6.3 (56, 4 H, Ar-H_o), 3.6 (s, THF), 1.4 (s, THF), 1.2 (23, 2 H, Ar-H_p), 0.6 (390, 12 H, *i*Pr-CH₃), -5.8 (18, 2 H, Ar-H_p), -10.1 (392, 12 H, *i*Pr-CH₃), -15.9 (17, 2 H, Ar-H_p) ppm.

A few drops of [D₅]pyridine were added to a solution of [DⁱppPhL]₂-Fe(THF) (14 mg, 0.01) in C₆D₆ (ca. 0.4 mL). The colour of the solution immediately changed to yellow. ¹H NMR (300 MHz, C₆D₆/C₅D₅N, 298 K): δ = 23.9 (20, 4 H, Ar-H_m), 16.9 (22, 4 H, Ar-H_m), 14.0 (26, 4 H, Ar-H_m), 8.4 (171, 4 H, Ar-H_o), 6.4 (83, 4 H, Ar-H_o), 3.6 (s, THF), 1.4 (s, THF), 1.3 (32, 2 H, Ar-H_p), 0.6 (390, 12 H, *i*Pr-CH₃), -5.8 (21, 2 H, Ar-H_p), -10.2 (329, 12 H, *i*Pr-CH₃), -15.7 (21, 2 H, Ar-H_p) ppm.

Pyridine (8 μL, 0.12 mmol) was added to a solution of [DⁱppPhL]₂-Fe(THF) (24.6 mg, 0.029 mmol) in C₆D₆ (ca. 0.4 mL). The colour of the solution changed from brown to orange/light brown. ¹H NMR (300 MHz, C₆D₆, 298 K): δ = 23.9 (34, 4 H, Ar-H_m), 17.0 (37, 4 H, Ar-H_m), 14.0 (40, 4 H, Ar-H_m), 11–6.7 (br., C₆D₅H and pyridine obscuring paramagnetic signals), 6.3, 3.6 (THF), 1.4 (THF), -5.8 (32, 2 H, Ar-H_p), -10.2 (384, 12 H, *i*Pr-CH₃), -15.7 (30, 2 H, Ar-H_p) ppm. Removal of the volatiles and redissolution in C₆D₆ resulted in a ¹H NMR spectrum identical to that obtained from reaction of **1c**·THF with 1 equiv. of pyridine.

Reaction of [DⁱppPhL]₂Fe(Et₂O) (1c·Et₂O) with [D₈]THF: A yellow solution of [DⁱppPhL]₂Fe(Et₂O) (15 mg, 0.02 mmol) in C₆D₆ (ca. 0.4 mL) in an NMR spectroscopy tube was reacted with a drop of [D₈]THF. The colour of the solution became slightly darker. ¹H NMR (300 MHz, C₆D₆, 298 K): similar to the ¹H NMR spectrum of **1c**·THF but without resonances at δ = 14.9 and 3.91 ppm (coordinated THF molecule). Free diethyl ether is observed at δ = 3.30 and 1.12 ppm.

Preparation of [DⁱppPhL]₂Fe(pyridine) (1c·py): Pyridine (0.1 mL, 1.23 mmol) was added to a brown solution of **1c**·Et₂O (0.36 g, 0.43 mmol) in toluene (15 mL). The colour changed to orange/light brown. The reaction mixture was stored at -80 °C for one day and

the product could be isolated as an orange powder (0.21 g, 60%). The ¹H NMR spectrum in C₆D₆ is identical to that obtained from the reaction of **1c**·THF with 1 equiv. pyridine as described above. C₅₅H₅₉FeN₅ (845.95): calcd. C 78.09, H 7.03, N 8.28; found C 76.60, H 6.60, N 7.86. IR (KBr): ν̄ = 3057, 1636, 1592, 1579, 1434, 1322, 1288, 1268, 1254, 1237, 1213, 1192, 1171, 1155, 1120, 1100, 1071, 1055, 1040, 1026, 997, 952, 936, 916, 896, 841, 804, 788, 766, 732, 699, 559, 536, 508 cm⁻¹.

Preparation of [DⁱppPhL]₂Fe(bpy) (1c·bpy): One equivalent of 2,2'-bipyridine (0.19 g, 1.192 mmol) was added to a yellow/brown solution of **1c**·Et₂O (1.00 g, 1.19 mmol) in toluene (about 10 mL) and an immediate change of colour to dark green was observed. The reaction mixture was reduced to about two thirds of its original volume and stored at -80 °C for one day. The product was isolated as dark green crystals; yield 0.703 g (0.765 mmol, 64%). ¹H NMR (300 MHz, C₆D₆, 298 K): δ (Δν_{1/2}, Hz): 112.6 (351, 1 H), 56.4 (66, 2 H, bpy), 43.6 (62, 2 H, bpy), 17.5 (277, 4 H, Ar-H_m), 15.2 (61, 8 H, 2 × Ar-H_o), 14.6 (53, 4 H, Ar-H_m), 13.1 (110, 2 H, bpy), 5.4 (36, 2 H, Ar-H_p), 4.4 (348, 12 H, *i*Pr-CH₃), 1.2 (46, 2 H, bpy), -3.1 (82, 12 H, *i*Pr-CH₃), -11.3 (36, 2 H, Ar-H_p), -16.1 (38, 2 H, Ar-H_p), -22.0 (256, 4 H, *i*Pr-CH) ppm. IR (KBr): ν̄ = 2137, 2070, 1779, 1632, 1595, 1580, 1315, 1260, 1237, 1190, 1151, 1111, 1098, 1077, 1058, 1024, 874, 804, 790, 767, 710, 698, 619, 597, 559, 530, 465 cm⁻¹. C₆₀H₆₂FeN₆ (C₇H₈)_{0.5} (969.11): calcd. C 78.70, H 6.86, N 9.10; found C 78.65, H 6.90, N 8.67.

Preparation of [C(O)N(Ph)C(Ph)NAr]₂Fe(CO)₂ (2): A solution of **1c**·Et₂O (313 mg, 37 mmol) in diethyl ether was degassed by three freeze-pump-thaw cycles. Afterwards an excess amount of CO (1 atm.) was admitted. The colour of the solution changed immediately from yellow to red. The reaction mixture was stirred for 3 d. Subsequently a yellow powder precipitated from the clear brown

Table 1. Crystal collection and refinement data.

	1c ·THF	1c ·Et ₂ O	1c ·bpy	2
Formula	C ₅₄ H ₆₂ N ₄ OFe	C ₅₄ H ₆₄ N ₄ OFe	C ₆₀ H ₆₂ FeN ₆	C ₅₄ H ₅₄ N ₄ O ₄ Fe
<i>M_r</i>	838.96	840.97	923.04	878.89
Dimensions [mm]	0.43 × 0.41 × 0.35	0.17 × 0.16 × 0.15	0.28 × 0.22 × 0.14	0.15 × 0.12 × 0.09
Colour, habit	yellow, block	yellow, parallelepiped	dark green, block	yellow, block
Crystal system	monoclinic	monoclinic	monoclinic	monoclinic
Space group, no. ^[24]	<i>P</i> 2 ₁ , 4	<i>P</i> 2 ₁ / <i>c</i> , 14	<i>P</i> 2 ₁ / <i>c</i> , 14	<i>P</i> 2 ₁ / <i>c</i> , 14
<i>a</i> [Å]	13.0056(5)	11.5817(7)	12.305(2)	13.9144(8)
<i>b</i> [Å]	18.6888(7)	23.119(1)	32.647(4)	18.004(1)
<i>c</i> [Å]	20.2539(8)	17.937(1)	15.802(2)	19.112(1)
β [°]	106.866(1)	98.933(1)	101.913(2)	98.649(1)
<i>Z</i>	4	4	4	4
<i>V</i> [Å ³]	4711.1(3)	4744.5(4)	6211.3(15)	4733.4(5)
ρ _{calcd.} [g cm ⁻³]	1.183	1.177	0.987	1.233
θ range [°]	2.18–28.28	2.30–25.02	2.29–23.53	2.26–25.03
λ [Å] (Mo- <i>K</i> _α)	0.71073	0.71073	0.71073	0.71073
<i>T</i> [K]	100(1)	100(1)	100(1)	200(1)
Collection time [h]	8.0	18.3	18	18.3
Measured reflections	43373	34022	38504	33835
Unique reflections	22725	8372	9223	8347
<i>M</i> [cm ⁻¹]	3.62	3.55	2.79	3.68
Parameters	1577	551	613	576
Weighting scheme <i>a</i> , <i>b</i> ^[a]	0.0496, 0.0	0.0420, 0.8754	0.1, 0.0	0.0435, 2.0026
<i>R</i> (<i>F</i>) for <i>F</i> _o ≥ 4σ(<i>F</i> _o) ^[b]	0.0375	0.0476	0.1184	0.0583
<i>wR</i> (<i>F</i> ²) ^[c]	0.0869	0.1098	0.2879	0.1399
Residual el. density [e Å ⁻³]	-0.23, 0.45(5)	-0.31, 0.45(5)	-0.6, 0.6(1)	-0.25, 0.38(6)
GoF ^[d]	1.006	1.011	1.155	1.010

[a] $w = 1/[\sigma^2(F_o^2) + (aP)^2 + bP]$, $P = [\max(F_o^2, 0) + 2F_c^2]/3$. [b] $R(F) = \Sigma(|F_o| - |F_c|)/\Sigma|F_o|$. [c] $wR(F^2) = \{\Sigma[w(F_o^2 - F_c^2)^2]/\Sigma[w(F_o^2)^2]\}^{1/2}$. [d] $\text{GoF} = \{\Sigma[w(F_o^2 - F_c^2)^2]/(n - p)\}^{1/2}$; *n* = number of reflections, *p* = number of parameters refined.

solution. The brown solution was decanted and the remaining yellow powder was dried in vacuo; yield 107 mg (0.12 mmol, 33%). The yield was not optimised. ¹H NMR (300 MHz, C₆D₆, 298 K): δ = 7.97 (d, *J* = 7.7 Hz, 2 H, Ar-CH), 7.07–6.45 (m, 24 H, Ar-CH), 3.64 (septet, *J* = 6.7 Hz, 2 H, *i*Pr-CH), 3.40 (septet, *J* = 6.7 Hz, 2 H, *i*Pr-CH), 1.63 (d, *J* = 6.6 Hz, 6 H, *i*Pr-CH₃), 1.45 (d, *J* = 7.0 Hz, 6 H, *i*Pr-CH₃), 1.27 (d, *J* = 7.0 Hz, 6 H, *i*Pr-CH₃), 1.11 (d, *J* = 6.6 Hz, 6 H, *i*Pr-CH₃) ppm. ¹³C{¹H} NMR (75 MHz, C₆D₆, 298 K): δ = 219.9 (C=O), 209.5 (C=O), 167.0 (NCN), 152.8, 148.7, 146.9, 135.0, 130.8 (5 × C_{ipso}), 129.3, 129.1, 129.0, 128.4, 127.3, 126.0, 125.6, 124.4, 124.2, 123.4 (10 × C_{Ar}, 3 resonances obscured by C₆D₆), 29.8, 28.9 (2 × *i*Pr-CH), 27.2, 26.8, 23.4, 22.8 (4 × *i*Pr-CH₃) ppm. IR (KBr): ν̄ = 3061 (w), 3023 (w), 2020 (s, C≡O), 1961 (s, C≡O), 1937 (w), 1659 (s, C=O), 1592 (m), 1584 (m), 1494 (w), 1321 (w), 1277 (w), 1186 (w), 1173 (w), 1102 (w), 1073 (w), 1040 (w), 1027 (w), 1003 (w), 989 (m), 930 (w), 898 (w), 796 (m), 761 (w), 743 (w), 706 (m), 693 (m), 652 (w), 598 (w), 579 (w), 544 (w), 470 (w), 449 (w) cm⁻¹. C₅₄H₅₄N₄O₄Fe (878.89): calcd. C 73.80, H 6.19, N 6.37; found C 73.71, H 6.13, N 6.44.

X-ray Diffraction: Crystals suitable for X-ray analysis were obtained at room temperature by layering a concentrated THF solution with hexanes (**1c**·THF), by layering a concentrated Et₂O solution with pentane (**1c**·Et₂O), by layering a toluene solution with pentane (**1c**·bpy) or by recrystallisation from toluene (**2**). Crystals were picked from the mother liquor and covered with inert oil to avoid deterioration due to loss of solvent from the crystal lattice. For **2**, the scattering power of the crystals was very weak: around half of the unique (till θ = 23.53°) merged reflections obey the *F*_o ≥ 4.0 σ(*F*_o) criterion of observability. This implies that the mean standard uncertainty (estimated standard deviation) is large compared to the mean magnitude of the (even more than double of the squared) structure factor. The weak scattering power might be the result of disorder. Refinement was also complicated by a disorder problem: from the solution it was clear that the solvate molecules were highly disordered and partly occupied. No satisfactory discrete model could be fitted in this density. The solvent contribution was taken into account using the SQUEEZE procedure in the PLATON program^[21] (1521.5 Å³ per unit cell). The program PLATON^[21] was used for geometrical analysis. Illustrations were generated using the programs ORTEP^[22] and POV-Ray^[23] (rendering).

Crystal collection and refinement data are given in (Table 1). CCDC-777666 (for ^{DippPh}LH), -777667 (for **1c**·THF), -777668 (for **1c**·Et₂O), -777669 (for **2**) and -777670 (for **1c**·bpy) contain the supplementary crystallographic data for this paper. These data can be obtained free of charge from The Cambridge Crystallographic Data Centre via www.ccdc.cam.ac.uk/data_request/cif.

Magnetic Measurements: Magnetic susceptibility measurements were performed on crystalline samples (ca. 25 mg) with a Quantum Design MPMS-7 SQUID magnetometer in the department of Solid State Chemistry at the University of Groningen. Samples were contained in sealed NMR spectroscopy tubes that were inserted into a plastic straw. Variable-temperature magnetisation data were collected at a field of 1000 G from 300 to 5 K with at least one data point every 5 K. The data were corrected for diamagnetism using Pascal's constants.^[25] Weiss constants (θ) were determined by least-square fits to the Curie–Weiss law; see Equation (1).

$$\chi = \frac{N_A g^2 \beta^2}{3k} \cdot \frac{S(S+1)}{T-\theta} \text{ in temperature regions } > 10\text{K} \quad (1)$$

Effective magnetic moments were calculated as Equation (2).

$$\mu_{\text{eff}} = 2.828 \sqrt{\chi_m T}, g = 2.00 \quad (2)$$

Zero-field splitting parameters were obtained by least-squares fitting of the observed susceptibility to the following Equation (3).^[26]

$$\chi = \frac{N_A g^2 \beta^2}{3kT} \left(\frac{2e^{-x} + 8e^{-4x} + \frac{12}{x}(1-e^{-x}) + \frac{8}{3x}(e^{-x} - e^{-4x})}{1 + 2e^{-x} + 2e^{-4x}} \right), x = D/kT \quad (3)$$

Supporting Information (see also the footnote on the first page of this article): X-ray structure of amidine ^{DippPh}LH, ¹H NMR spectra for reactions of **1b** with pyridine and magnetic susceptibility data for **1c**·bpy.

- [1] S. Hao, S. Gambarotta, C. Bensimon, J. J. H. Edema, *Inorg. Chim. Acta* **1993**, *213*, 65–74.
- [2] A. R. Sadique, M. J. Heeg, C. H. Winter, *J. Am. Chem. Soc.* **2003**, *125*, 7774–7775.
- [3] a) R. T. Boeré, V. Klassen, G. Wolmershäuser, *J. Chem. Soc., Dalton Trans.* **1998**, 4147–4154; b) R. T. Boeré, M. L. Cole, P. C. Junk, *New J. Chem.* **2005**, *29*, 128–134.
- [4] C. A. Nijhuis, E. Jellema, T. J. J. Sciarone, A. Meetsma, P. H. M. Budzelaar, B. Hessen, *Eur. J. Inorg. Chem.* **2005**, 2089–2099.
- [5] J. R. Hagadorn, J. Arnold, *Inorg. Chem.* **1997**, *36*, 132–133.
- [6] J. A. R. Schmidt, J. Arnold, *J. Chem. Soc., Dalton Trans.* **2002**, 3454.
- [7] B. S. Lim, A. Rahtu, J.-S. Park, R. G. Gordon, *Inorg. Chem.* **2003**, *42*, 7951–7958.
- [8] B. Vendemiati, G. Prini, A. Meetsma, B. Hessen, J. H. Teuben, O. Traverso, *Eur. J. Inorg. Chem.* **2001**, 707–711.
- [9] H. Kawaguchi, T. Matsuo, *Chem. Commun.* **2002**, 958–959.
- [10] E. Otten, P. Dijkstra, C. Visser, A. Meetsma, B. Hessen, *Organometallics* **2005**, *24*, 4374–4386.
- [11] The adduct **1c**·THF crystallises with two independent molecules in the asymmetric unit. In view of their geometric similarity, only one of these is discussed here.
- [12] A. W. Addison, T. Nageswara Rao, J. Reedijk, J. van Rijn, G. C. Verschoor, *J. Chem. Soc., Dalton Trans.* **1984**, 1349–1356.
- [13] H. K. Lee, T. S. Lam, C.-K. Lam, H.-W. Li, S. M. Fung, *New J. Chem.* **2003**, *27*, 1310–1318.
- [14] R. Boča, *Coord. Chem. Rev.* **2004**, *248*, 757–815.
- [15] M. L. Cole, P. C. Junk, *New J. Chem.* **2005**, *29*, 135–140.
- [16] J. R. Hagadorn, J. Arnold, *J. Organomet. Chem.* **2001**, *637*–639, 521–530.
- [17] T. J. J. Sciarone, C. A. Nijhuis, A. Meetsma, B. Hessen, *Organometallics* **2008**, *27*, 2058–2065.
- [18] T. J. J. Sciarone, C. A. Nijhuis, A. Meetsma, B. Hessen, *Dalton Trans.* **2006**, 4896–4909.
- [19] C. Jones, C. Schulten, R. P. Rose, A. Stasch, S. Aldridge, W. D. Woodul, K. S. Murray, B. Moubarak, M. Brynda, G. La Macchia, L. Gagliardi, *Angew. Chem. Int. Ed.* **2009**, *48*, 7406–7410.
- [20] P. Kovacic, N. O. Brace, *Inorg. Synth.* **1960**, *6*, 172–173.
- [21] a) A. L. Spek, PLATON – Program for the automated analysis of molecular geometry (A multipurpose crystallographic tool), University of Utrecht, The Netherlands, **2002**; b) A. L. Spek, *Acta Crystallogr., Sect. A* **1990**, *46*, C34.
- [22] Ortep-3 for Windows: L. J. Farrugia, *J. Appl. Crystallogr.* **1997**, *30*, 565.

- [23] Rendering was made with POV-Ray 3.6, Persistence of Vision Pty. Ltd. (2004), Persistence of Vision Raytracer (version 3.6), retrieved from <http://www.povray.org/download/>.
- [24] *International Tables for Crystallography*, Kluwer Academic Publishers, Dordrecht, The Netherlands, 1992.
- [25] O. Kahn, *Molecular Magnetism*, VCH Publishers, New York, 1993, p. 3.
- [26] C. J. O'Connor, *Magnetochemistry – Advances in Theory and Experimentation*, in: *Progress in Inorganic Chemistry*, Wiley, New York, 1982, pp. 203–283.

Received: June 30, 2010

Published Online: December 3, 2010